Ordered intracellular RecA–DNA assemblies: A potential site of *in vivo* RecA-mediated activities

Smadar Levin-Zaidman*, Daphna Frenkiel-Krispin*, Eyal Shimoni*, Ilana Sabanay*, Sharon G. Wolf†, and Abraham Minsky*‡

*Department of Organic Chemistry, and †Electron Microscopy Center, Weizmann Institute of Science, Rehovot 76100, Israel

Edited by Charles M. Radding, Yale University School of Medicine, New Haven, CT, and approved March 9, 2000 (received for review December 8, 1999)

The inducible SOS response increases the ability of bacteria to cope with DNA damage through various DNA repair processes in which the RecA protein plays a central role. Here we present the first study of the morphological aspects that accompany the SOS response in *Escherichia coli*. We find that induction of the SOS system in wild-type bacteria results in a fast and massive intracellular coaggregation of RecA and DNA into a lateral macroscopic assembly. The coaggregates comprise substantial portions of both the cellular RecA and the DNA complement. The structural features of the coaggregates and their relation to *in vitro* RecA–DNA networks, as well as morphological studies of strains carrying RecA mutants, are all consistent with the possibility that the intracellular assemblies represent a functional entity in which RecA-mediated DNA repair and protection activities occur.

biocrystallization | DNA repair | homology search | stress response

RecA-mediated DNA recombination and repair processes proceed through several sequential phases (1–3). A presynaptic filament in which RecA molecules coat a single-stranded DNA substrate is initially formed. The filament acts then as a sequence-specific DNA-binding entity, capable of searching and binding dsDNA sites that are homologous to the RecA-coated segment. Within the resulting joint species, DNA strand exchange and heteroduplex extension processes are promoted. The mechanism that enables a rapid search for DNA homology *in vivo*, within a highly crowded and complex genome, remains enigmatic.

To reach its target, any sequence-specific DNA-binding protein must overcome two general obstacles: a minute cellular concentration of the target, and a vast excess of nontarget, yet still competitive, DNA sites. The search for a homologous DNA site conducted by the RecA–DNA presynaptic filament shares these hurdles, but is further encumbered by the uniquely adverse diffusion characteristics of its components. A DNA target corresponds to a segment that is part of, and embedded within, the chromosome. This, and the large structural asymmetry of DNA, conspire to minimize the diffusion constant of DNA sites (4, 5). In a homology search executed by the RecA–DNA filament, both the searching and the target entities are chromosomal DNA sites whose small diffusion constants drastically attenuate their encounter rate. How then does a RecA-mediated intracellular search evade the kinetic impediments that are intrinsic to the nature of its components?

Here we show that damages inflicted on bacterial DNA lead to a rapid formation of an ordered intracellular assembly that accommodates both RecA and DNA. We suggest that the striated morphology of this RecA–DNA assembly is capable of promoting an *in vivo* homology search by attenuating both the sampling volume and the dimensionality of the process. Moreover, RecA was shown to protect chromosomal DNA from degradation (6) through unknown mechanisms. The tight crystalline packaging that is progressively assumed by the intracellular RecA–DNA assemblies as DNA damages accumulate is proposed to confer efficient DNA protection through physical sequestration.

Materials and Methods

Electron Microscopy. Wild-type *Escherichia coli* AB1157 (*recA*$^+$, *lexA*$^+$) as well as various *recA* mutants were grown in LB medium without NaCl to midlogarithmic phase. Cultures were then either treated with 100 μg of nalidixic acid or exposed to UV irradiation (20 J/m^2, 254 nm). After incubation at 37°C for 15, 30, 60, 90, or 120 min, cells were fixed by ultrafast freezing in liquid ethane and cryosubstituted as described (7). Three independent experiments were conducted for each time point, and in each experiment, 800–1,000 cell slices were screened. In control experiments, chemical fixation was performed according to the RK-U procedure (8). Samples were embedded in Epon; thin sections were stained with 1% uranyl acetate and examined on a Philips CM12 electron microscope operating at 100 kV.

***In Situ* Localization of DNA and RecA.** Intracellular localization of DNA was performed with the DNA-specific stain osmium-ammine-SO_2 (9). Grid-mounted thin sections of Epon-embedded bacteria were floated on 5 M HCl for 30 min at room temperature, washed with distilled water, and treated with osmium ammine-B (Polysciences) in 8 M acetic acid/40 mM sodium metabisulfite for 1 h at 37°C. Sections were then thoroughly rinsed with distilled water, dried, and studied without additional staining.

The intracellular distribution of RecA was determined by immunogold labeling. Grid-mounted thin sections were incubated for 1 h on a saturated aqueous solution of sodium periodate and then treated with blocking solution (1% goat serum/1% gelatin/0.5% BSA in PBS) for 1 h. Grids were then incubated for 2 h with rabbit IgG anti-RecA polyclonal antibodies (1:200 dilution with PBS). After a wash with the blocking solution, grids were incubated with gold-conjugated goat anti-rabbit IgG for 1 h, dried, and stained with 2% uranyl acetate. All transactions were performed at room temperature.

Image Reconstruction. Images of the intracellular crystals were digitized with an Imacon Flextight scanner. Processing included crystal "unbending" and averaging with the MRC IMAGE software (10). The density maps were prepared with the CCP4 program suite.

Results

Morphological Reorganization in DNA-Damaged Bacteria. Bacterial chromatin is demarcated in electron micrographs of metabolically active cells as amorphous ribosome-free spaces that are irregularly spread over the cytoplasm (7, 8) (Figs. 1*A* and 2*A*).

This paper was submitted directly (Track II) to the PNAS office.

Abbreviations: dsDNA, double-stranded DNA.

‡To whom reprint requests should be addressed. E-mail: avi.minsky@weizmann.ac.il.

The publication costs of this article were defrayed in part by page charge payment. This article must therefore be hereby marked "*advertisement*" in accordance with 18 U.S.C. §1734 solely to indicate this fact.

Article published online before print: *Proc. Natl. Acad. Sci. USA*, 10.1073/pnas.090532397. Article and publication date are at www.pnas.org/cgi/doi/10.1073/pnas.090532397

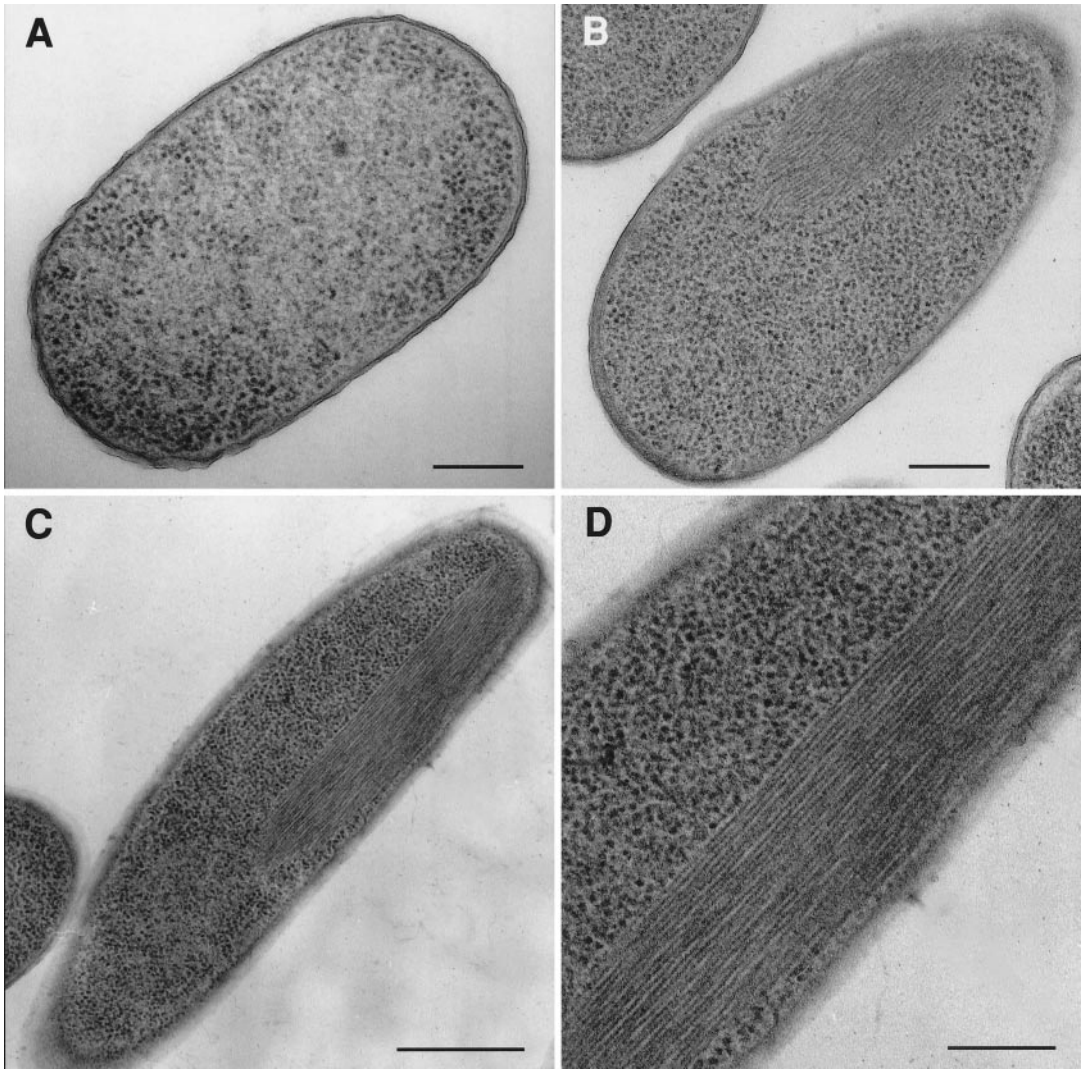

Fig. 1. Electron microscopy of *E. coli* exposed to DNA-damaging agents. (*A*) Wild-type *E. coli* AB1157 at midlogarithmic phase. The dark particles are ribosomes. The ribosome-free spaces contain chromatin. (*B*) AB1157 cells treated with nalidixic acid for 30 min. A similar morphology is exhibited by UV-irradiated bacteria. (*C*) Cells treated with nalidixic acid in the presence of spermidine (2.5 mM) for 2 h. (*D*) High magnification of the assembly shown in *C*. Identical morphologies are detected in bacteria fixed by either cryo or chemical methods. Because these two fixation modes proceed through fundamentally different mechanisms, detection of the assemblies in both procedures indicates that these structures represent a genuine morphological feature. (Scale bars are 200 nm in *A*, *B*, and *D*, and 500 nm in *C*.)

Wild-type *E. coli* cells exposed to DNA-damaging agents that induce the SOS response reveal a strikingly different morphology (Fig. 1*B*). In bacteria treated with nalidixic acid, which effects double-strand DNA breaks by stalling the activity of DNA gyrase (11), the DNA-containing ribosome-free regions can no longer be discerned. Instead, the ribosomes appear to be uniformly distributed over the cytoplasm. The redistribution of ribosomes, and hence of chromatin, is accompanied by the appearance of a prominent array of parallel bundles. Continuous treatment of the cells with nalidixic acid leads to a progressive expansion of the assembly, whose average length increases from 200 nm after 15 min to 800 ± 100 nm after 60 min. Further incubation does not affect a significant expansion but results in a higher lateral order, as indicated by the appearance of diffraction patterns. The average distance between bundles derived from these patterns is 10 nm. At this stage, the lateral assembly occupies a fifth of the cell volume, as deduced from measurements on several hundred bacterial sections. Notably, when the dimension of the assemblies is a fifth of the cell volume, they should statistically be detected in a fifth of the very thin randomly cut cell slices, if present in all cells. Indeed, 25 ± 5 assemblies are found per 100 cells sections, indicating that they are formed in a vast majority of stressed bacteria.

Similar morphological traits, including the appearance of a lateral assembly and the redistribution of ribosomes, are also detected shortly after exposure of wild-type bacteria to a UV pulse. Further unstressed incubation results in a rapid disappearance of the assembly, indicating that the stress-induced effects are reversible. Significantly, UV irradiation causes DNA lesions in a replication-dependent pathway that is fundamentally different from the DNA-damaging mechanism of nalidixic acid (12). Thus, the massive intracellular reorganization represents a generic outcome of SOS-inducing DNA lesions.

Positively charged polyamines promote the morphological modifications that are sustained by wild-type bacteria treated with DNA-damaging factors. Addition of spermidine to the growth media before the treatment with nalidixic acid or after UV irradiation accelerates the redistribution of ribosomes into

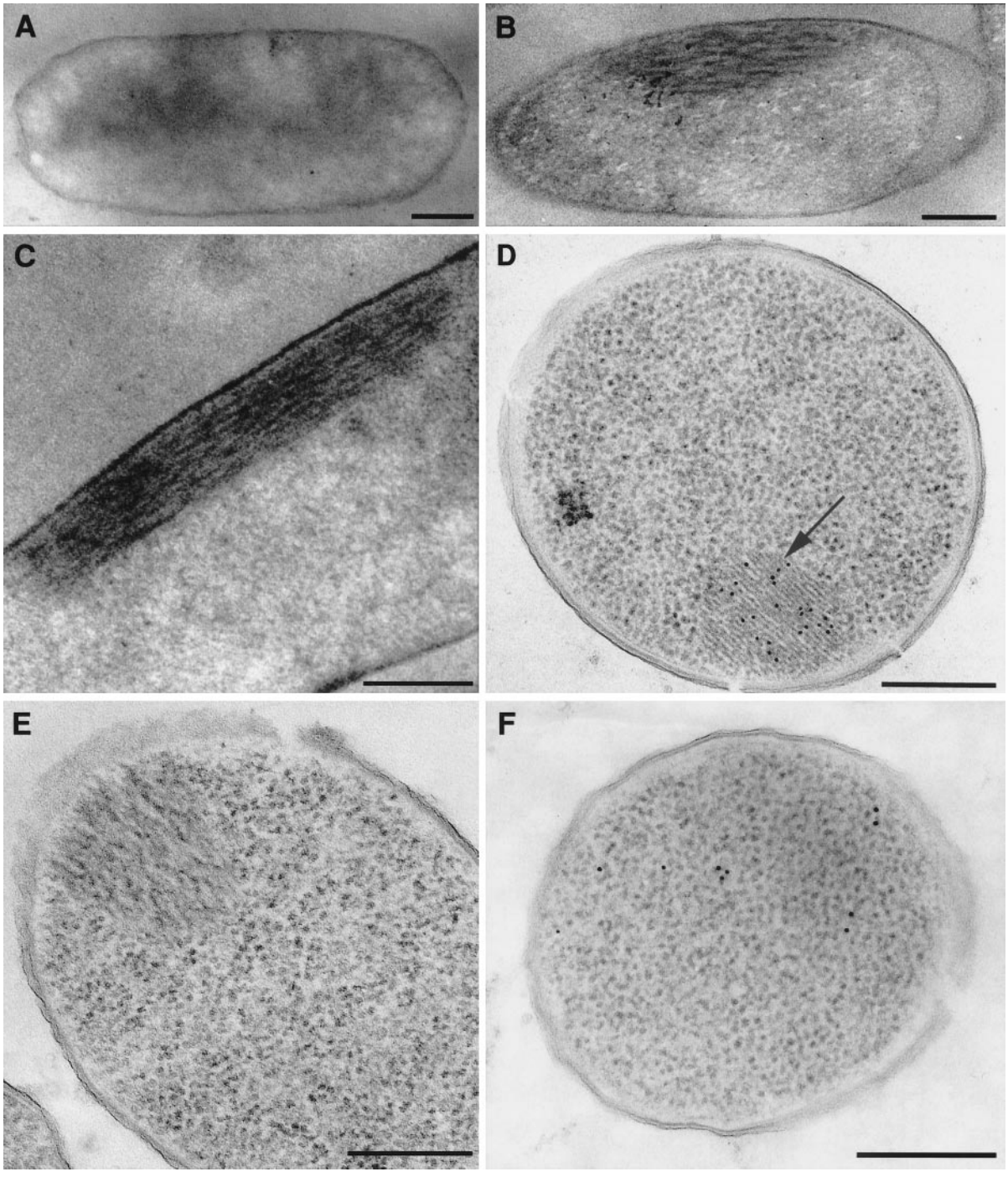

Fig. 2. *In situ* localization of DNA and RecA. (*A*) Wild-type *E. coli* AB1157 cells at midlogarithmic phase, stained *solely* with the DNA-specific reagent osmium-ammine-SO_2. The irregular spreading of chromatin over the cytoplasm is indicated. (*B* and *C*) Identical staining, but after treatment of bacteria with nalidixic acid for 60 min. (*D*) Immunogold labeling of AB1157 cells exposed to nalidixic acid for 60 min, by using anti-RecA antibodies and gold-conjugated IgG (detected as electron-dense dots). Exclusive localization of RecA within the ordered assembly (highlighted by an arrow) is noted. (*E*) *RecA423* bacteria (15) treated with nalidixic acid and spermidine for 2 h. (*F*) Immunogold labeling with anti-RecA antibodies of *RecA428* cells (14) exposed to nalidixic acid and spermidine for 2 h. (Scale bars are 250 nm.)

a uniform organization and the formation of a striated array. Whereas both the size and order of the assemblies increase in the presence of spermidine (Figs. 1 *C* and *D*; and 3), the average interfiber distance of 10 nm remains the same as for the assemblies formed without the polyamine. Unstressed bacteria grown in the presence of spermidine, for periods identical to those used for SOS induction, do not exhibit morphological modifications.

Nalidixic acid-treated or UV-exposed Δ*RecA* bacteria, in which the *RecA* gene has been knocked-out, fail to reveal the above described morphological patterns. Similarly, no morphological modulations can be detected in stressed bacteria carrying the RecA mutants RecA1 and RecA13 that are highly deficient in their ability to elicit SOS response as well as to bind dsDNA molecules (13). After exposure to DNA-damaging agents, the morphology of the Δ*RecA, RecA1*, and *RecA13* strains remains

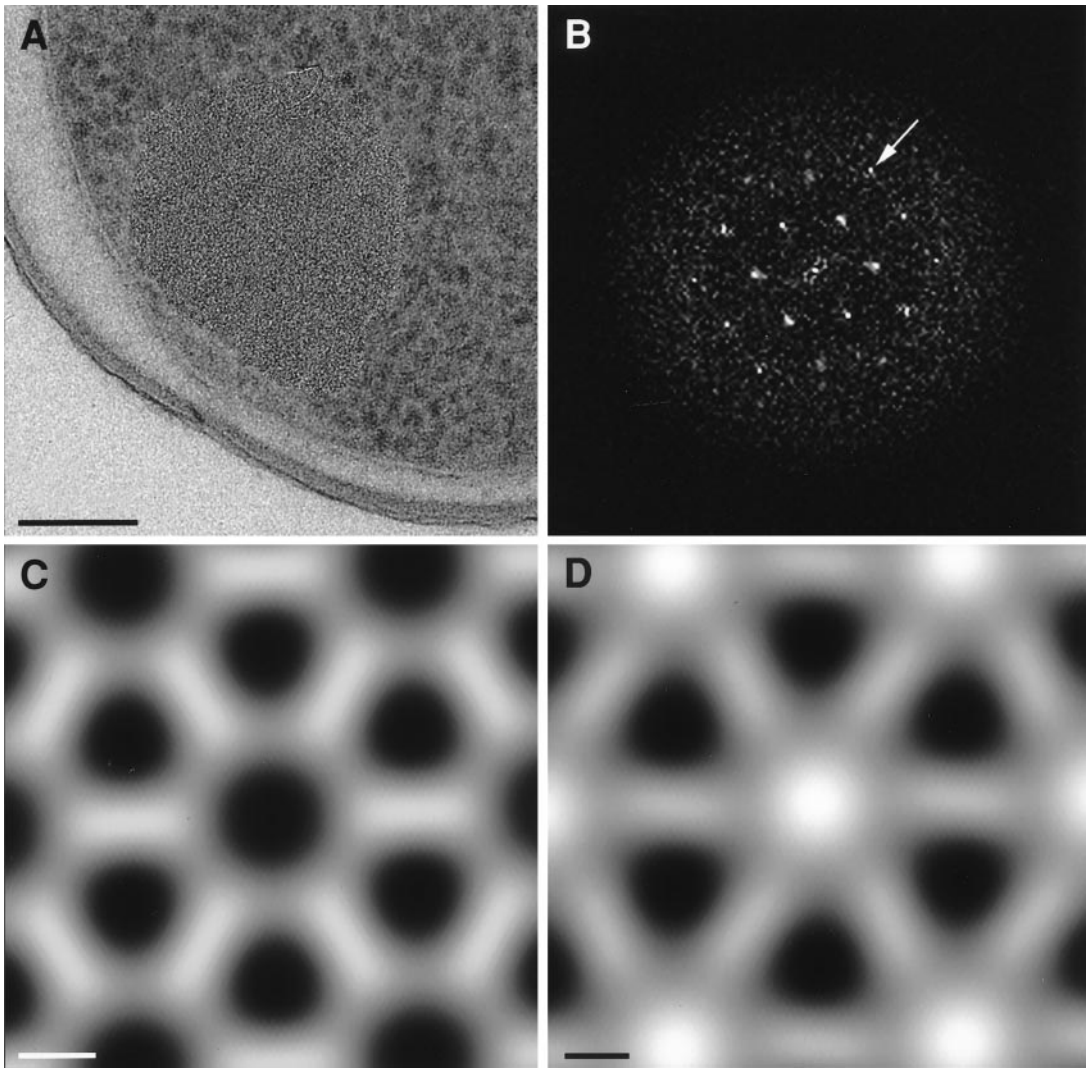

Fig. 3. Cross-sectional views and image reconstruction of intracellular RecA–DNA assemblies. (*A*) Cross-sectional view of a RecA–DNA assembly exhibited by *E. coli* treated for 2 h with nalidixic acid and spermidine. (Scale bar is 50 nm.) (*B*) Calculated Fourier transform of the intracellular assembly shown in *A*. Arrow indicates reflection at 47Å resolution. (*C*) Projection map along the *z* axis of RecA crystal obtained *in vitro* in the absence of DNA (16), centered on a RecA filament. (*D*) Density map of the intracellular crystal, derived from the *in vivo* crystal shown in *A*. (Scale bars in *C* and *D* are 30 Å.)

indistinguishable from that exhibited by nonstressed wild-type cells (Fig. 1*A*).

Intracellular Assemblies Consist of RecA and DNA. To assess the composition of the striated assembly exhibited by bacteria exposed to DNA-damaging agents, labeling studies that allow intracellular localization of dsDNA and the RecA protein were performed. Application of the DNA-specific stain osmium-ammine (9) on electron microscopy sections of nonstressed bacteria reveals the characteristic random distribution of bulk chromatin over the cytoplasm (Fig. 2*A*). In sharp contrast, nalidixic acid-treated cells exhibit heavy staining that colocalizes with the striated assembly (Fig. 2 *B* and *C*), thus indicating massive DNA packaging within this assembly. The cellular distribution of RecA was probed by immunogold labeling, by using anti-RecA antibodies. A study of 300–400 immunogold-labeled specimens indicates that RecA molecules are confined to the striated assembly (Fig. 2*D*). No labeling was observed when anti-RecA antibodies were used to probe nonstressed wild-type cells or nalidixic acid-treated Δ*RecA* bacteria.

The notion that the intracellular assemblies contain both RecA and DNA was further tested by using two strains carrying the RecA mutants *RecA423* and *RecA428* (14, 15). RecA423 contains a single-point mutation (Arg-169 → His) which is located near the L1 loop, and RecA428 carries a single mutation (Gly-200 → Asp) at the L2 loop. These two loops were suggested to be involved in DNA binding (16). In contrast to the RecA1 and RecA13, RecA423 and RecA428 induce the SOS response and are constitutively expressed, and hence are present in large amounts within the cells. Yet, RecA423 (15) and, in particular, RecA428 (A. Bailone, personal communication) reveal substantially attenuated rates of DNA binding and are severely impaired in promoting recombinational DNA repair. After prolonged exposure of the *RecA423* strain to SOS-inducing DNA-damaging agents, only small and disordered assemblies are observed (Fig. 2*E*). No RecA–DNA coaggregation can be detected in *RecA423* bacteria that have not been exposed to DNA-damaging agents. The *RecA428* strain reveals a particularly severe phenotype; cells expressing this mutant are as defective in DNA repair as are Δ*RecA* bacteria (14). Indeed, although present in substantial amounts within the cells (as indicated by immunogold labeling), RecA428 molecules remain scattered over the cytoplasm and do

not form RecA–DNA assemblies even after prolonged exposure of the cells to DNA-damaging agents, in either the absence or presence of spermidine (Fig. 2*F*).

The periodic order exhibited by the intracellular assemblies obtained after prolonged exposure of wild-type bacteria to nalidixic acid (Fig. 3 *A* and *B*) is high enough to allow crystallographic averaging. The projection density map derived from the *in vivo* organization (Fig. 3*D*) is compared with the *in vitro* P6-symmetry packing of the RecA crystal obtained in the absence of DNA (16) (Fig. 3*C*). The resolution of the RecA crystal has been reduced to 35 Å to match that of the *in vivo* RecA–DNA assembly. The two projections are practically identical, apart from one major disparity. At the site of the sixfold axis, a large buildup of density is detected in the intracellular crystal, whereas in the RecA crystal, the corresponding region is empty space.

Discussion

E. coli cells exposed to environmental assaults that lead to dsDNA breaks are found to form an ordered macroscopic assembly that contains DNA and RecA molecules. This coaggregate may represent either a RecA storage form, or the actual site where RecA-mediated activities occur. Although the observations reported above do not allow discrimination between these alternatives, they strongly support the notion that the intracellular RecA–DNA coaggregate is mechanistically linked to RecA-mediated repair and protection activities.

The intracellular assemblies are formed in a wild-type strain, in which RecA expression is effected as an inherent step of the physiological response to DNA damage. Notably, the assemblies consist of filaments that contain DNA (Fig. 3*D*). It is generally accepted that RecA–DNA interactions activate RecA and induce the SOS response (12). Thus, RecA molecules within the RecA–DNA intracellular complexes are likely to be in their active form. The coaggregate appears shortly after exposure of wild-type *E. coli*, but not of Δ*RecA*, *RecA1*, or *RecA13* strains, to DNA-damaging agents. Because DNA damages accumulate, the size of the coaggregate progressively increases, and it rapidly dissipates as the SOS response ends. Thus, coaggregation is reversible, its extent corresponds to the severity of the applied assault and its temporal parameters match those of the SOS response. This correspondence is at odds with the notion that the assemblies represent a nonfunctional storage form. Because substantial portions of the RecA cellular pool is localized within the aggregate, it is unlikely that RecA-dependent activities occur outside of the assembly. Moreover, the notion that cells exposed to an acute assault respond by segregating an essential repair protein within an inactive form that also incorporates a large portion of their DNA complement, is hard to conceive.

The results obtained from the *RecA423* and *RecA428* strains are particularly suggestive. Both mutants exhibit a constitutive LexA-coprotease activity, thus being constitutively expressed, and are as proficient as the wild-type protein in eliciting the SOS response. Yet, because of their dramatically reduced rates of DNA binding, they are severely deficient in promoting homologous repair (14, 15). The low frequency or complete absence of ordered assemblies in these strains implies that the mere presence, even at large amounts, of RecA molecules is not sufficient for the formation of the assemblies. Rather, RecA activation through specific RecA–DNA interactions are required, thus supporting a correlation between the assemblies and RecA-mediated repair activities. Notably, RecA inclusion bodies have been observed in a strain that heavily overproduces RecA under conditions that do not cause DNA lesions (17). These structures do not incorporate DNA and represent a storage form. Thus, intracellular RecA self-aggregation may occur, but only under nonnative conditions of massive overproduction. The promoting effect exerted by polyamines on the order and rate of formation of the assembly is also indicative. Spermidine was found to stimulate the formation of active RecA–DNA presynaptic filaments by facilitating the removal of the competing single-stranded-binding protein (18). Spermidine was also shown to promote crystallization of purified RecA (19). Finally, coaggregates are invariably found adjacent to the cell membrane. Indeed, RecA–membrane association has been argued to be related to RecA activation through its binding to DNA (20). On the basis of these observations, we propose that the intracellular RecA–DNA coaggregate represents the *in vivo* site where RecA-mediated DNA repair activities occur.

In vitro RecA-mediated homologous pairing exhibits Michaelis-Menten-type kinetics, where the rate-limiting step is the conversion to products of a complex composed of RecA–DNA presynaptic filaments and dsDNA molecules (21–23). Large RecA–DNA coaggregates have indeed been detected by sedimentation (24–26) and *in vitro* electron microscopy (27), and were suggested to represent an intermediate on the pathway to homologous alignment (25, 26). Presumably, such coaggregates, held together by transient protein–protein, protein–DNA, and DNA–DNA interactions, act to reduce the sampling volume. An increase in the effective DNA concentration has indeed been shown to accelerate DNA catenation (28) and renaturation processes (29).

We propose that the intracellular assemblies represent a functional analog of the *in vitro* RecA–DNA networks. Being completely disordered (27), the *in vitro* networks cannot, however, alter the dimensionality of the search (30). In contrast, the intracellular assemblies may promote a homology search by *both* an attenuated sampling volume that results from RecA–DNA coaggregation, and a reduced dimensionality which specifically stems from the longitudinal organization of the *in vivo* assembly. Within such a linear, yet nondiffracting, loosely packed and fluid array, composed of chromosomal RecA–DNA filaments and dsDNA, a translational motion is facilitated by geometrical constraints. Thus, instead of sampling the genome through a three-dimensional random drift, RecA–DNA presynaptic filaments may search for homologous sites by a one-dimensional slide along the dsDNA, whose parallel arrangement coincides with the main axis of the assembly. On the basis of a mutational analysis of RecA (31, 32) and its crystal structure (16), it was proposed that RecA–DNA filaments and dsDNA molecules align to form a functional bundle-like coaggregate (32). This model is consistent with the striated morphology of the intracellular assembly (Figs. 1 and 2). It is also consistent with the redistribution of chromatin that accompanies RecA–DNA coaggregation in DNA-damaged bacteria, which implies that DNA is being progressively pulled out from ribosome-free regions where it resides in nonstressed cells into the RecA–DNA complex (Fig. 2 *A–C*).

On continuous exposure of bacteria to DNA-damaging agents, the loosely packed wavy assemblies that are detected after UV pulses or short exposure periods to nalidixic acid (Fig. 1*B*), progressively assume a tight morphology whose crystalline nature is indicated by the appearance of diffraction patterns (Fig. 3*A*). Presumably, the accumulation of stable joints between presynaptic filaments and homologous dsDNA segments after continuous stress, results in an attenuated fluidity of the assemblies, thus enhancing their compactness and order. The additional density detected in the *in vivo* projection map (Fig. 3*D*) in comparison to the map of the *in vitro* RecA crystal (Fig. 3*C*), could be accounted for by the presence of DNA as well as by RecA DNA-binding loops (16). Notably, the 10-nm interfilament spacing, measured from both the assembly side views (Fig. 1) and from the projection map (Fig. 3*D*), is consistent with the *in vitro* filament diameter (33, 34).

The crystalline morphology that characterizes RecA–DNA assemblies in bacteria that have sustained prolonged exposure to DNA-damaging agents is, however, intriguing. Such a tight

organization cannot be reconciled with dynamic search and repair processes. We submit that when DNA damages become extensive, the intracellular assemblies progressively assume a protective role, acting to physically shield the DNA molecules. Double-stranded DNA segments within RecA-mediated homologous joints were indeed shown to be protected against DNA-modifying enzymes (35). Moreover, complete degradation of chromosomes was observed in Δ*RecA* cells (6). In a recent study, we showed that DNA protection is effected in starved bacteria by cocrystallization of their DNA with the stress-induced protein Dps (36). We propose that RecA–DNA biocrystallization represents an additional example of a "last resort" protection strategy that becomes operative under continuous stress, and involves physical sequestration of DNA within crystalline assemblies.

DNA repair processes occur in all living systems. Rad51, the eukaryotic homolog of RecA, forms protein–DNA filaments similar to the RecA–DNA presynaptic complex (37), and promotes homologous pairing and strand exchange (38). At the onset of meiotic prophase, Rad51 foci on the chromatin coalesce into large linear arrays (39, 40) that were proposed to comprise multiple Rad51–DNA filaments bound to many dsDNA sequences (40). Notably, the Rad51 foci are induced by DNA damages and colocalize with DNA repair sites that were coined repairosomes (41). The general similarity between the striated RecA–DNA coaggregates and the eukaryotic repairosomes is intriguing. It may imply that similar mechanisms, which critically depend on specific morphological traits, are used throughout the living kingdom to overcome the unique hurdles that are intrinsic to the DNA homology search. Thus, it is tempting to suggest that the evolutionary conservation of the recombination machinery (38) derives in part from stringent morphological requirements that are imposed by genome-wide search processes.

We thank Z. Livneh for the generous gift of anti-RecA antibodies, and A. Bailone for the *RecA423* and *RecA428* strains. We also wish to thank E. Kellenberger for his help with the cryofixation technique. This work was supported by the Israel Science Foundation founded by the Academy of Sciences and Humanities, and the Minerva Foundation (Germany).

1. Kowalczykowski, S. C. (1991) *Annu. Rev. Biophys. Biophys. Chem.* **20,** 539–575.
2. Kowalczykowski, S. C., Dixon, D. A., Eggleston, A. K., Lauder, S. D. & Rehrauer, W. M. (1994) *Microbiol. Rev.* **58,** 401–465.
3. Roca, A. I. & Cox, M. M. (1997) *Prog. Nucleic Acid Res. Mol. Biol.* **56,** 129–223.
4. Berg, O. G., Winter, R. B. & von Hippel, P. H. (1981) *Biochemistry* **20,** 6929–6948.
5. von Hippel, P. H. & Berg, O. G. (1989) *J. Biol. Chem.* **264,** 675–678.
6. Skarstad, K. & Boye, E. (1993) *J. Bacteriol.* **175,** 5505–5509.
7. Hobot, J. A., Villiger, W., Escaig, J., Maeder, M., Ryter, A. & Kellenberger, E. (1985) *J. Bacteriol.* **162,** 960–971.
8. Robinow, C. & Kellenberger, E. (1994) *Microbiol. Rev.* **58,** 211–232.
9. Vazquez-Nin, G. H., Biggiogera, M. & Echeverria, O. M. (1995) *Eur. J. Histochem.* **39,** 101–106.
10. Crowther, R. A., Henderson, R. & Smith, J. M. (1996) *J. Struct. Biol.* **116,** 9–16.
11. Reece, R. J. & Maxwell, A. (1991) *Crit. Rev. Biochem. Mol. Biol.* **26,** 335–375.
12. Sassanfar, M. & Roberts, J. W. (1990) *J. Mol. Biol.* **212,** 79–96.
13. Kowalczykowski, S. C. (1991) *Biochimie* **73,** 289–304.
14. Asai, T., Sommer, S., Bailone, A. & Kogoma, T. (1993) *EMBO J.* **12,** 3287–3295.
15. Ishimori, K., Sommer, S., Bailone, A., Takahashi, M., Cox, M. M. & Devoret, R. (1996) *J. Mol. Biol.* **264,** 696–712.
16. Story, R. M., Weber, I. T. & Steitz, T. A. (1992) *Nature (London)* **355,** 318–325.
17. Ruigrok, R. W., Bohrmann, B., Hewat, E., Engel, A., Kellenberger, E. & DiCapua, E. (1993) *EMBO J.* **12,** 9–16.
18. Wei, T. F., Bujalowski, W. & Lohman, T. M. (1992) *Biochemistry* **31,** 6166–6174.
19. Griffith, J. & Shores, C. G. (1985) *Biochemistry* **24,** 158–162.
20. Garvey, N., St. John, A. C. & Witkin, E. M. (1985) *J. Bacteriol.* **163,** 870–876.
21. Gonda, D. K. & Radding, C. M. (1983) *Cell* **34,** 647–654.
22. Gonda, D. K., Shibata, T. & Radding, C. M. (1985) *Biochemistry* **24,** 413–420.
23. Yancey-Wrona, J. E. & Camerini-Otero, R. D. (1995) *Curr. Biol.* **5,** 1149–1158.
24. Chow, S. A. & Radding, C. M. (1985) *Proc. Natl. Acad. Sci. USA* **82,** 5646–5650.
25. Gonda, D. K. & Radding, C. M. (1986) *J. Biol. Chem.* **261,** 13087–13096.
26. Tsang, S. S., Chow, S. A. & Radding, C. M. (1985) *Biochemistry* **24,** 3226–3232.
27. Pinsince, J. M. & Griffith, J. D. (1992) *J. Mol. Biol.* **228,** 409–420.
28. Krasnow, M. A. & Cozzarelli, N. R. (1982) *J. Biol. Chem.* **257,** 2687–2693.
29. Sikorav, J.-L. & Church, G. M. (1991) *J. Mol. Biol.* **222,** 1085–1108.
30. Adzuma, K. (1998) *J. Biol. Chem.* **273,** 31565–31573.
31. Benedict, R. C. & Kowalczykowski, S. C. (1988) *J. Biol. Chem.* **263,** 15513–15520.
32. Liu, S. K., Eisen, J. A., Hanawalt, P. & Tessman, I. (1993) *J. Bacteriol.* **175,** 6518-6529.
33. Yu, X. & Egelman, E. H. (1997) *Nat. Struct. Biol.* **4,** 101–104.
34. Egelman, E. H. & Stasiak, A. (1986) *J. Mol. Biol.* **191,** 677–697.
35. Ferrin, L. J. & Camerini-Otero, R. D. (1991) *Science* **254,** 1494–1497.
36. Wolf, S. G., Frenkiel, D., Arad, T., Finkel, S. E., Kolter, R. & Minsky, A. (1999) *Nature (London)* **400,** 83–85.
37. Ogawa, T., Yu, X., Shinohara, A. & Egelman, E. H. (1993) *Science* **259,** 1896–1899.
38. Baumann, P. & West, S. C. (1998) *Trends Biochem. Sci.* **23,** 247–251.
39. Barlow, A. L., Benson, F. E., West, S. C. & Hulten, M. A. (1997) *EMBO J.* **16,** 5207- 5215.
40. Plug, A. W., Xu, J., Reddy, G., Golub, E. I. & Ashley, T. (1996) *Proc. Natl. Acad. Sci. USA* **93,** 5920–5924.
41. Haaf, T., Raderschall, E., Reddy, G., Ward, D. C., Radding, C. M. & Golub, E. I. (1999) *J. Cell Biol.* **144,** 11–20.